OL | Organic Letters

Letter

Cite This: Org. Lett. 2019, 21, 4433−4438

pubs.acs.org/OrgLett

Design, Synthesis, and Conformational Analysis of Oligobenzanilides as Multifacial α-Helix Mimetics

Theo Flack, Charles Romain, Andrew J. P. White, Peter R. Haycock, and Anna Barnard*

Department of Chemistry, Molecular Sciences Research Hub, Imperial College London, London W12 0BZ, U.K.

Supporting Information

ABSTRACT: The design, synthesis, and conformational analysis of an oligobenzanilide helix mimetic scaffold capable of simultaneous mimicry of two faces of an α-helix is reported. The synthetic methodology provides access to diverse monomer building blocks amenable to solid-phase assembly in just four synthetic steps. The conformational flexibility of model dimers was investigated using a combination of solid and solution state methodologies supplemented with DFT calculations. The lack of noncovalent constraints allows for significant conformational plasticity in the scaffold, thus permitting it to successfully mimic residues *i*, *i*+2, *i*+4, *i*+6, *i*+7, and *i*+9 of a canonical α-helix.

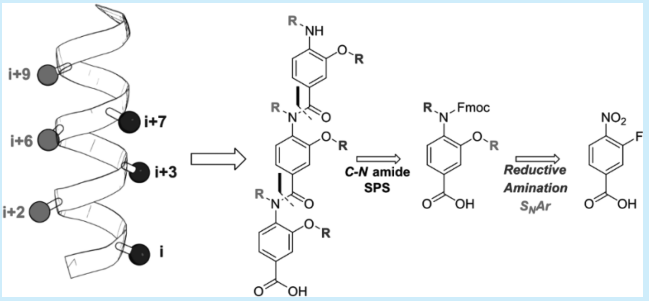

Protein−protein interactions (PPIs) are central to all biological processes and offer a vast array of potential therapeutic targets.[1−3] However, selective targeting of protein−protein interfaces remains an enormous challenge. In comparison to the small, well-defined pocket of an enzyme−substrate interaction (300−500 Å^2), the interface of a typical PPI is large (1000−2000 Å^2) and topographically featureless.[4,5] The most common molecular recognition scaffold in multiprotein complexes is the α-helix, and as such, numerous strategies to target this class of PPI using rationally designed molecules have been reported, including both peptidic and nonpeptidic approaches, a concept known as peptidomimetics.[6,7]

Typically, helix mimetics possess two common features: a rigid scaffold to mimic the rod-like morphology of the helical backbone and side chains to recapitulate the spatial orientation of hotspot residues on the native helix.[8] The majority of scaffolds reported have focused on mimicry of key recognition residues located on a single face of an α-helix (*i*, *i*+3/4, and *i*+7).

However, given that roughly one-third of PPIs interact through more than one helical face, there is an obvious requirement for helix mimetics that simultaneously mimic more than one helical face.[9] Embellishment of previously reported scaffolds has resulted in multifacial helix mimetics such as *bis*- and *tris*-benzamides, and benzoylureas and novel scaffolds such as diphenylacetylenes and azaoctanes have also been developed (Figure 1).[10−15]

Common to all two-faced helix mimetics published are lengthy, complex syntheses that limit their potential as generic tools for PPI inhibition. As part of our interest in developing methods to inhibit complex protein−protein interactions, we sought to design a novel synthetically accessible two-faced α-helix mimetic scaffold. Given the prevalence of oligobenzamide

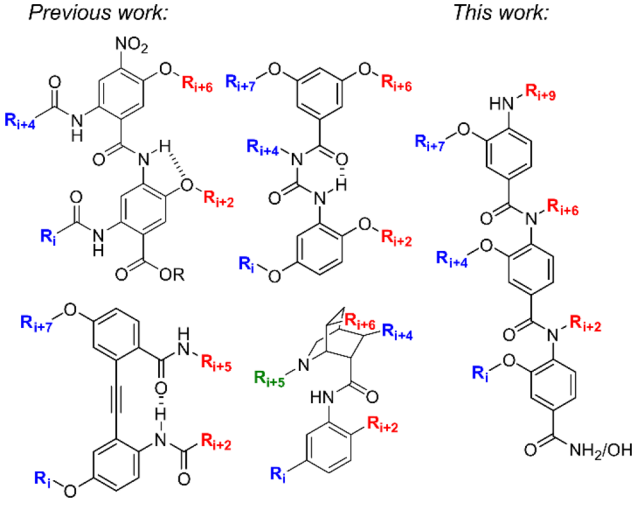

Figure 1. Previously published multifacial α-helix mimetics: *bis*-benzamides, benzoylureas, diphenylacetylenes, azaoctanes, and our novel oligobenzanilide.

scaffolds, we chose to develop a two-faced scaffold based upon this linkage. Herein, we describe the design, synthesis, and conformational analysis of a novel 3-*O*-alkyated, 4-*N*-dialkylated helix mimetic that is capable of simultaneously mimicking residues *i*, *i*+2, *i*+4, *i*+6, *i*+7, and *i*+9 of a canonical α-helix.

Our novel scaffold was designed by combining two previously published scaffolds onto a single helix mimetic: Wilson's *N*-alkylated triaryl amide and Boger's 3-*O*-alkylated

Received: March 29, 2019
Published: June 12, 2019

DOI: 10.1021/acs.orglett.9b01115
Org. Lett. 2019, 21, 4433−4438

triaryl amide were combined to give a 3-*O*-,4-*N*-dialkylated scaffold capable of simultaneous mimicry of two helical faces (Figure 1).[16,17] The synthetic route to the individual monomers is shown in Scheme 1. Notable features of the

Scheme 1. Synthesis of Fmoc-Protected Monomers

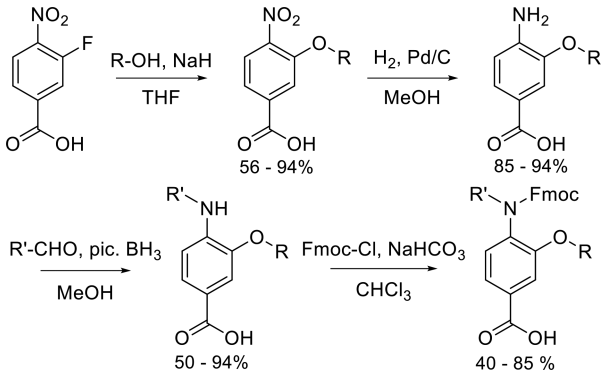

synthetic route are (i) a common starting material to access most monomers, (ii) compatibility with the Fmoc/^{t}Bu protocol for solid-phase synthesis (SPS), and (iii) the wide variety of functionality, both natural and unnatural, that may be incorporated at both positions on the individual monomers.

3-Fluoro-4-nitrobenzoic acid was used as the starting material for monomer synthesis. The nitro group simultaneously activates the 3′-position for nucleophilic aromatic substitution and "protects" the aniline required for installation of the second side chain and subsequent coupling reactions. Using this S_NAr approach, it is possible to incorporate functionality found across the majority of proteinogenic amino acids as well as the enormous chemical space that has not been sampled by nature. For most monomers, catalytic hydrogenation afforded the primary aniline in near quantitative yields. For monomers with functionality susceptible to hydrogenation, a tin(II) chloride-based reduction was used. The second side chain was introduced onto the primary aniline through a one-pot reductive amination using a picoline–borane complex (pic-BH_3) as the stoichiometric reductant. All aldehydes corresponding to hydrophobic amino acids side chains are commercially available. Unoptimized yields for these hydrophobic aldehydes were typically >80%. Aldehydes for installation of polar side chains were typically obtained by oxidation of the hydroxycarbamate to the aldehyde with Dess–Martin periodinane.

To render the monomers compatible with Fmoc/^{t}Bu SPS, the secondary anilines were Fmoc protected to afford the tertiary amide in reasonable yields (40–70%). Using this four-step protocol, we generated a library of 13 diverse monomers containing charged, polar, and hydrophobic functionality in both positions (Table 1 and Figure S1).

In comparison to previously published helix mimetics, oligomers were assembled by loading the monomers directly onto a solid support (Scheme 2). HATU mediated coupling under microwave heating allowed the Fmoc-protected monomers to be loaded onto a rink amide resin, whereas monomers could be loaded on a 2-chlorotrityl resin at room temperature by stirring with DIPEA. To effect amide bond formation, the benzoic acid was activated *in situ* to the acyl chloride using Ghosez's reagent in anhydrous *N*-methyl-2-pyrollidone (NMP) according to previously published methodology (Scheme 3).[18] Products were isolated by mass-directed

Table 1. 3-*O*, 4-*N*-Dialkylated Monomers Synthesized

compound no.	R	R'	yield (%)
1	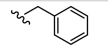		27
2			46
3			56
4			15
5			30
6			8
7		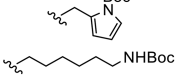	32
8		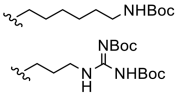	14
9	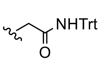		30
10	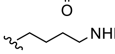		17
11	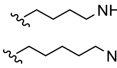		42
12	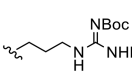		35
13	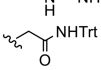	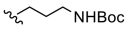	34

Scheme 2. Monomer Resin Loading

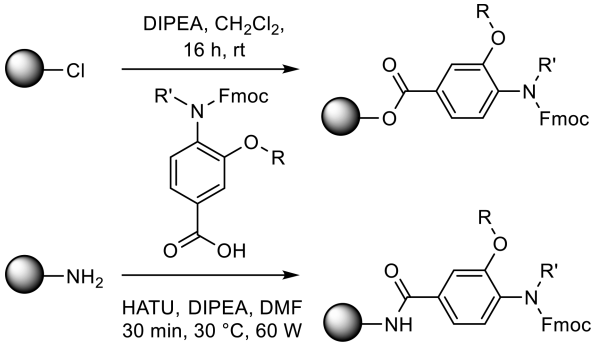

purifications. To exemplify the methodology, three dimers and two trimers were successfully produced bearing a range of hydrophobic and polar side chains (Figures 2 and S2 and Table 2).

It is well established that *N*-alkylated benzanilides preferentially adopt a "folded" conformation about the amide bond in which the aryl rings are *cis* (formally *E*/*s*-*trans*).[19−21]

Clearly, a permanent *cis* relationship about the amide bond is not representative of the elongated structure of the α-helix and as such is unlikely to lead to effective perturbation of α-helix-mediated PPIs. However, the *N*-alkylated benzanilide scaffolds have been shown to be as potent as both (i) the native peptide and (ii) benzamide scaffolds with preorganization endowed through intramolecular hydrogen bonding networks.[16]

To study the conformational space of our scaffold, we selected a triage of *ab initio,* solution-, and solid-state techniques. For ease of analysis, representative dimers **14**–**16** were chosen as model compounds for experimental studies. These dimers (Figure 2) contain all the features common to more extended oligomers: (i) a central amide linkage and thus the potential for *cis*–*trans* isomers, (ii) the potential for *syn*/*anti* conformers with regards to the *O*-alkoxy substituent, and

DOI: 10.1021/acs.orglett.9b01115
Org. Lett. 2019, 21, 4433−4438

Scheme 3. Solid Phase Oligomer Synthesis

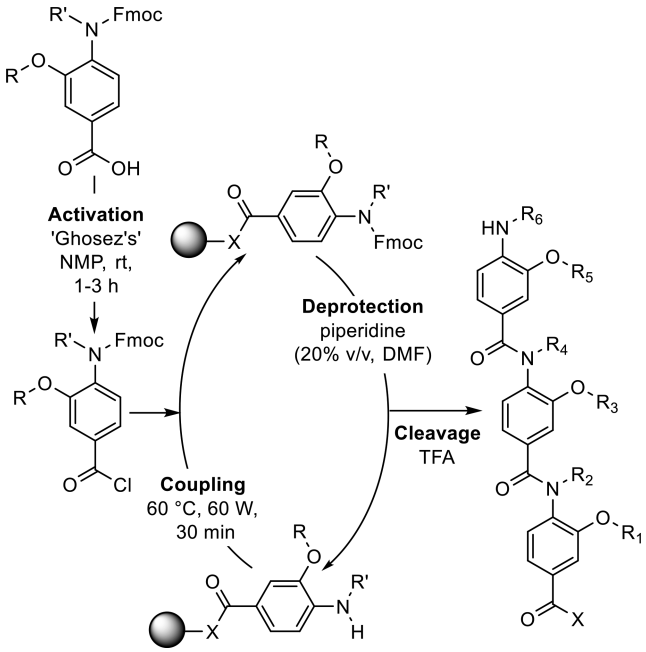

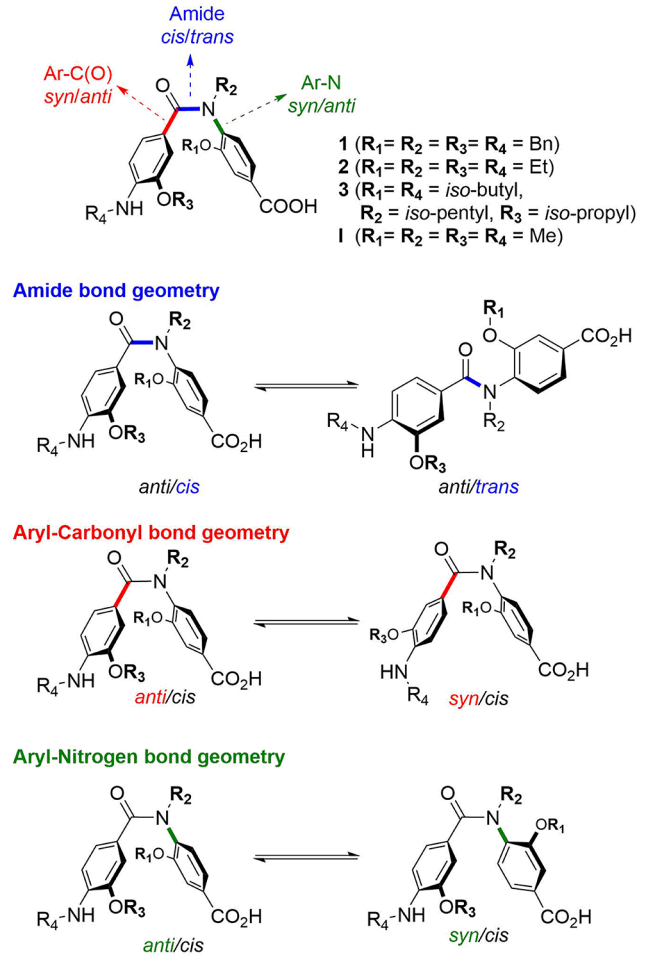

Figure 2. 3-*O*, 4-*N*-Dialkylated benzanilide dimers synthesized and the conformational and stereochemical isomerization available to the helix mimetic scaffold.

(iii) the potential for restricted rotation about the aryl-nitrogen (Ar−N) bond.

Single crystals suitable for X-ray diffraction of compound **16** were generated by slow evaporation of a solution of hexane:ethyl acetate (1:1). The unit cell contained two chemically identical but crystallographically independent structures (Figure 3). As expected, both structures clearly demonstrate the *cis*-isomer about the amide bond with the two 3-*O*-substituents on opposing faces, presumably minimizing unfavorable steric clashes. $A^{1,3}$ strain between phenyl rings results in the aromatic rings lying roughly perpendicular to the plane of the amide bond with the aromatic rings partially facing each other. This perpendicular *cis-anti* conformer is consistent with previous solid-state structures of tertiary benzanilides.[22] Interestingly, the amide bond displays a significant distortion from planarity (12.1° for **16-A**, 16.3° for **16-B**, Table S1) placing the latter within the top 5% of the acyclic amides in which the amide bond is not constrained with a ring (nonlactam).

An important feature highlighted by the solid-state structure is the presence of axial chirality. Restricted rotation about the Ar−N axis of benzanilides is long known, and many *ortho*-substituted anilides displaying axial chirality have been documented.[22−25] This bond rotation in helix mimetics is significant in allowing scope for side chains to recapitulate native interactions through an induced-fit binding mechanism. In multifacial helix mimetics, rotation about the Ar−N bond corresponds to interconversion between helical faces (Figure 2).

To calculate the barrier to rotation about the Ar−N bond, variable temperature (VT) NMR spectroscopy was used. Given rotation about the Ar−N bond of unsymmetrically substituted anilides interconverts not only enantiomeric conformers but diastereotopic protons, it is possible to measure the rate of, and therefore barrier to, rotation. The ^{1}H NMR spectra of **14**−**16** at 298 K in DMSO-d_6 all displayed a single set of broadened resonances indicative of an exchange process but with no distinction between the putative diastereotopic protons (Figure S3). This is indicative of "fast" exchange in solution at room temperature.

To investigate the nature of the exchange, low temperature NMR spectra were taken at the slow-exchange limit. As expected, equal intensity signal doubling due to restricted rotation about the Ar−N axis was observed. For dimers **14**, **15**, and **16**, anisochronicity was observed for all methylene protons on the 3-*O*-alkoxy and amide substituents (spin-systems: **14** = AB; **15** = ABX_3; **16** = varies). In addition, dimer **3** demonstrated diastereotopic methyl doublets (spin-system = AX_3X_3'). For all dimers studied, no magnetic inequivalence was observed for protons on the secondary aniline substituent due to the increased distance from the chiral Ar−N axis.

Modeling the coalescence of the methylene protons in dimer **14** gave a barrier to rotation of 14.9 kcal mol^{-1} ± 0.59. For dimer **16**, modeling the coalescence of the methyl doublets gave a barrier to rotation of 13.9 kcal mol^{-1} ± 0.41 (Figures 4, S4, and S5). Both values correspond to an estimated millisecond half-life for racemization. Thus, although interconversion between enantiomers is slow on the NMR time scale, the helix mimetic scaffold is not atropisomeric at room temperature (Oki's definition >1000 s at 25 °C[26]), and as such, the "helical" faces mimicked by the scaffold are interconverting rapidly at 298 K and thus sample a vast array of conformational space. Unfortunately, spectral crowding prevented us from

DOI: 10.1021/acs.orglett.9b01115
Org. Lett. 2019, 21, 4433−4438

Table 2. 3-*O*, 4-*N*-Dialkylated Benzanilide Dimers and Trimers Synthesized

compound no.	R_1	R_2	R_3	R_4	R_5	R_6	yield (%)
14	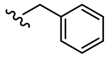	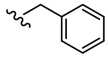	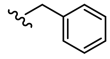	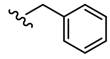	N/A	N/A	4
15					N/A	N/A	23
16		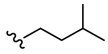			N/A	N/A	40
17						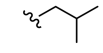	10
18	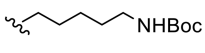	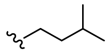	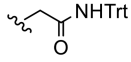		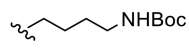	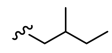	3

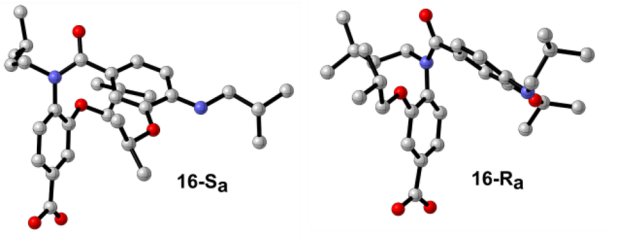

Figure 3. X-ray structures of **16** (**16**-S_a and **16**-R_a).

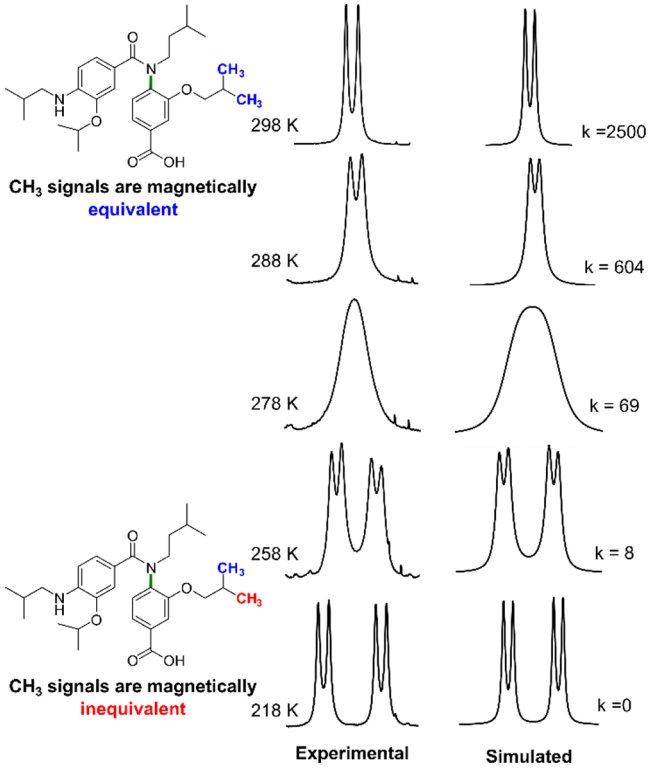

Figure 4. Experimental and simulated NMR spectrum of **16** at the slow-exchange limit.

obtaining accurate energies for Ar−N bond rotation for compound **15**.

2D NOESY and selNOE experiments at 298 K revealed through-space correlations characteristic of a *cis* conformation about the central amide bond (Figure S6), in line with a fast exchange at room temperature and existence of *cis* conformations. However, no characteristic correlation showing existence of a *trans* conformation was observed by 2D NMR spectroscopy, presumably due to the large distance (>5 Å) between the two aromatic moieties of interest in the *trans* conformation.

To further explore the barriers to rotation about the Ar−N and amide bonds, DFT calculations were carried out, and energy barriers of the rotations about the amide, Ar−C(O) and Ar−N bonds were calculated based on methods previously used by Miller[27] (details in Supporting Information). A simplified model dimer was used in which all alkyl groups were replaced by methyl groups (**I**, Figure 2). Rotations solely about the amide bond were found to have energy barriers as low as ΔG_{298} = 14.1 kcal/mol (**I-TS2**, Figures 5, S12, and S15)

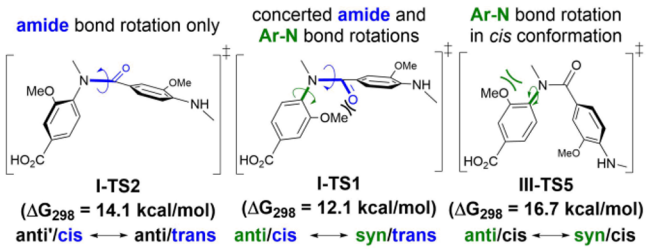

Figure 5. Examples of energy barriers ΔG_{298} for selected bond rotations (see details in the Supporting Information)

and only led to *cis*/*trans* conformational exchanges (i.e., no *anti*/*syn* conformational exchange, Figures S12 and S15). Interestingly, as previously reported by others,[27−29] concerted amide and Ar−N bond rotations occurred with slightly lower energy barriers of ΔG_{298} = 12.1 kcal/mol (**I-TS1**, Figures 5, S10, and S19) and led to concerted *cis*/*anti* and *syn*/*trans* conformational exchanges (i.e. *anti*/*cis* ↔ *syn*/*trans* or *syn*/*cis* ↔ *anti*/*trans*, Figures S10 and S19). These concerted rotations are a consequence of the amide carbonyl oxygen and the *ortho*-*O*-alkoxy group of the benzamide "pushing" each other during the rotations (Figure 5). Rotations about the Ar−C(O) bond were found to occur with low energy barriers ΔG_{298} < 10 kcal/mol for both *trans* and *cis* conformations about the amide bond (Figures S21 and S22). Finally, rotations about the Ar−N bond in a *cis* conformation were found to have the highest energy barrier ΔG_{298} = 16.7 kcal/mol due to a steric clash between the *ortho*-*O*-alkoxy group of the benzamide and the *N*-Me group of the amide moiety (**III-TS5**, Figure 5).

Numerous pathways are possible for the exchange between the two crystallographically observed enantiomers. However,

DOI: 10.1021/acs.orglett.9b01115
Org. Lett. 2019, 21, 4433−4438

exchange between the two enantiomers via constant *cis* conformations is likely to be the least favorable pathway due to the high energy barrier of the Ar−N bond rotation (Figure 5). Alternatively, pathways via extended conformations are more favorable, involving bond rotations with lower energy barriers with a maximum of 14.1 kcal/mol (Figure S30), in good agreement with the experimental values of 14.9 and 13.9 kcal/mol.

The Boltzmann population of both conformers was calculated based on the energy required for rotation about the amide bond or Ar−N bond or a concerted rotation (Table S15). Given the energy difference between the *cis* and *trans* conformations, it is not surprising to find that at equilibrium, >99% of the scaffold exists in the folded conformation at 298 K. However, this does not preclude the molecule from adopting a *trans* conformation. The low energy barriers associated with these bond rotations strongly suggests that our scaffold can sample an extended "helix mimetic" conformation at room temperature.

We described the design, synthesis, and conformational analysis of a novel oligo 3-*O*, 4-*N*-dialkylated benzanilide helix mimetic scaffold capable of simultaneous mimicry of side chains *i*, *i*+2, *i*+4, *i*+6, *i*+7, and *i*+9 of a canonical α-helix. The synthetic route is the shortest and most straightforward described to date for multifacial helix mimetics. A combination of solid-state, solution-phase, and *in silico* analyses show that the helix mimetic scaffold rapidly samples a wide variety of conformations in solution and can successfully mimic the relevant helical pharmacophore. The increased conformational plasticity in comparison with previous helix mimetic design is a shift for the proteomimetic field. To this date, the analysis of helix mimetics has focused on reporting RMSD values obtained from energy-minimized or solid-state structures. As noted by Burgess, it is evident that this is not representative of the equilibrating conformations present in solution.[30−32] This work goes part way to demonstrating that a more sophisticated approach to characterization of helix mimetics is required if the values are to be considered a determinant in the quality of a scaffold. Furthermore, a degree of conformational plasticity has been noted to be advantageous for protein−surface recognition through an induced-fit-type mechanism. This is even more pertinent given that most secondary structure elements at protein interfaces are perturbed from geometric ideality. Future work on this scaffold will focus initially on inhibition of complex helix−protein interactions that are mediated by the binding of more than one helical face. For example, malaria parasite invasion of host red blood cells is critically dependent on the fully buried interaction which exists between myosin tail interacting protein (MTIP) and myosin A (MyoA),[33] and in oncology, the Wnt signaling pathway is centered around β-catenin, which forms multifacial PPIs with T-cell factor 4 (Tcf-4)[34] and B cell lymphoma 9 (BCL9).[35]

■ ASSOCIATED CONTENT

Supporting Information

The Supporting Information is available free of charge on the ACS Publications website at DOI: 10.1021/acs.orglett.9b01115.

Supplementary figures, experimental procedures, compound characterization, copies of ^{1}H and ^{13}C NMR spectra, computational figures, and experimental procedures (PDF)

Accession Codes

CCDC 1902316 contains the supplementary crystallographic data for this paper. These data can be obtained free of charge via www.ccdc.cam.ac.uk/data_request/cif, by emailing data_request@ccdc.cam.ac.uk, or by contacting The Cambridge Crystallographic Data Centre, 12 Union Road, Cambridge CB2 1EZ, UK; fax: +44 1223 336033. Complementary FAIR data[36] are available from the Imperial College Data Repository at DOI: 10.14469/hpc/5108.

■ AUTHOR INFORMATION

Corresponding Author

*E-mail: a.barnard@imperial.ac.uk.

ORCID

Charles Romain: 0000-0002-1851-8612
Anna Barnard: 0000-0002-1327-3417

Notes

The authors declare no competing financial interest.

■ ACKNOWLEDGMENTS

The authors thank Dr. Lisa Haigh, Imperial College London for mass spectrometry and Prof. Ed Tate, Imperial College London for support and advice. A.B. and C.R. thank Imperial College London for their Junior Research Fellowships. A.B. would like to thank the Wellcome Trust for funding for her JRF (Grant 105603/Z/14/Z).

■ REFERENCES

(1) Arkin, M. M. R.; Wells, J. a. Small-Molecule Inhibitors of Protein-Protein Interactions: Progressing towards the Dream. *Nat. Rev. Drug Discovery* **2004**, *3* (4), 301−317.

(2) Arkin, M. R.; Tang, Y.; Wells, J. A. Small-Molecule Inhibitors of Protein-Protein Interactions: Progressing toward the Reality. *Chem. Biol.* **2014**, *21* (9), 1102−1114.

(3) Stumpf, M. P. H.; Thorne, T.; de Silva, E.; Stewart, R.; An, H. J.; Lappe, M.; Wiuf, C. Estimating the Size of the Human Interactome. *Proc. Natl. Acad. Sci. U. S. A.* **2008**, *105* (19), 6959−6964.

(4) Fuller, J. C.; Burgoyne, N. J.; Jackson, R. M. Predicting Druggable Binding Sites at the Protein-Protein Interface. *Drug Discovery Today* **2009**, *14* (3−4), 155−161.

(5) Hwang, H.; Vreven, T.; Janin, J.; Weng, Z. Protein-Protein Docking Benchmark Version 4.0. *Proteins: Struct., Funct., Genet.* **2010**, *78* (15), 3111−3114.

(6) Bullock, B. N.; Jochim, A. L.; Arora, P. S. Assessing Helical Protein Interfaces for Inhibitor Design. *J. Am. Chem. Soc.* **2011**, *133* (36), 14220−14223.

(7) Azzarito, V.; Long, K.; Murphy, N. S.; Wilson, A. J. Inhibition of Alpha-Helix-Mediated Protein-Protein Interactions Using Designed Molecules. *Nat. Chem.* **2013**, *5* (3), 161−173.

(8) Clackson, T.; Wells, J. A. A Hot Spot of Binding Energy in a Hormone-Receptor Interface. *Science* **1995**, *267* (5196), 383−386.

(9) Jochim, A. L.; Arora, P. S. Assessment of Helical Interfaces in Protein-Protein Interactions. *Mol. BioSyst.* **2009**, *5* (9), 924−926.

(10) Jayatunga, M. K. P.; Thompson, S.; Hamilton, A. D. Alpha-Helix Mimetics: Outwards and upwards. *Bioorg. Med. Chem. Lett.* **2014**, *24* (3), 717−734.

(11) Marimganti, S.; Cheemala, M. N.; Ahn, J. M. Novel Amphiphilic α-Helix Mimetics Based on a Bis-Benzamide Scaffold. *Org. Lett.* **2009**, *11* (19), 4418−4421.

(12) Thompson, S.; Vallinayagam, R.; Adler, M. J.; Scott, R. T. W.; Hamilton, A. D. Double-Sided α-Helix Mimetics. *Tetrahedron* **2012**, *68* (23), 4501−4505.

DOI: 10.1021/acs.orglett.9b01115
Org. Lett. 2019, 21, 4433−4438

(13) Thompson, S.; Hamilton, A. D. Amphiphilic α-Helix Mimetics Based on a Benzoylurea Scaffold. *Org. Biomol. Chem.* **2012**, *10* (30), 5780−5782.
(14) Jung, K. Y.; Vanommeslaeghe, K.; Lanning, M. E.; Yap, J. L.; Gordon, C.; Wilder, P. T.; Mackerell, A. D.; Fletcher, S. Amphipathic α-Helix Mimetics Based on a 1,2-Diphenylacetylene Scaffold. *Org. Lett.* **2013**, *15* (13), 3234−3237.
(15) Bayly, A. R.; White, A. J. P.; Spivey, A. C. Design and Synthesis of a Prototype Scaffold for Five-Residue α-Helix Mimetics. *Eur. J. Org. Chem.* **2013**, *2013* (25), 5566−5569.
(16) Campbell, F.; Plante, J. P.; Edwards, T. A.; Warriner, S. L.; Wilson, A. J. N-Alkylated Oligoamide α-Helical Proteomimetics. *Org. Biomol. Chem.* **2010**, *8* (10), 2344−2351.
(17) Shaginian, A.; Whitby, L. R.; Hong, S.; Hwang, I.; Farooqi, B.; Searcey, M.; Chen, J.; Vogt, P. K.; Boger, D. L. Design, Synthesis, and Evaluation of an a-Helix Mimetic Library Targeting Protein-Protein Interactions. *J. Am. Chem. Soc.* **2009**, *131* (15), 5564−5572.
(18) Murphy, N. S.; Prabhakaran, P.; Azzarito, V.; Plante, J. P.; Hardie, M. J.; Kilner, C. A.; Warriner, S. L.; Wilson, A. J. Solid-Phase Methodology for Synthesis of O-Alkylated Aromatic Oligoamide Inhibitors of α-Helix-Mediated Protein-Protein Interactions. *Chem. - Eur. J.* **2013**, *19* (18), 5546−5550.
(19) Itai, A.; Toriumi, Y.; Tomioka, N.; Kagechika, H.; Azumaya, I.; Shudo, K. Stereochemistry of N-Methylbenzanilide and Benzanilide. *Tetrahedron Lett.* **1989**, *30* (45), 6177−6180.
(20) Campbell, F.; Plante, J.; Carruthers, C.; Hardie, M. J.; Prior, T. J.; Wilson, A. J. Macrocyclic Scaffolds Derived from P-Aminobenzoic Acid. *Chem. Commun.* **2007**, No. 22, 2240−2242.
(21) Saito, S.; Toriumi, Y.; Tomioka, N.; Itai, A. Theoretical Studies on Cis-Amide Preference in N-Methylanilides. *J. Org. Chem.* **1995**, *60* (15), 4715−4720.
(22) Adler, T.; Bonjoch, J.; Clayden, J.; Font-Bardía, M.; Pickworth, M.; Solans, X.; Solé, D.; Vallverdú, L. Slow Interconversion of Enantiomeric Conformers or Atropisomers of Anilide and Urea Derivatives of 2-Substituted Anilines. *Org. Biomol. Chem.* **2005**, *3* (17), 3173−3183.
(23) Siddall, T. H.; Prohaska, C. A. Geminal Proton Non-equivalences and Related Phenomena in Some N-Substituted Amides. *J. Am. Chem. Soc.* **1966**, *88* (6), 1172−1176.
(24) Shvo, Y.; Taylor, E. C.; Mislow, K.; Raban, M. Chemical Shift Nonequivalence of Diastereotopic Protons Due to Restricted Rotation Around Aryl-Nitrogen Bonds in Substituted Amides. *J. Am. Chem. Soc.* **1967**, *89* (19), 4910−4917.
(25) Chabaud, L.; Clayden, J.; Helliwell, M.; Page, A.; Raftery, J.; Vallverdú, L. Conformational Studies of Tertiary Oligo-m-Benzanilides and Oligo-p-Benzanilides in Solution. *Tetrahedron* **2010**, *66* (34), 6936−6957.
(26) Ōki, M. Recent Advances in Atropisomerism. *Top. Stereochem.* **1983**, 1−81.
(27) Barrett, K. T.; Metrano, A. J.; Rablen, P. R.; Miller, S. J. Spontaneous Transfer of Chirality in an Atropisomerically Enriched Two-Axis System. *Nature* **2014**, *509* (7498), 71−75.
(28) Clayden, J.; Pink, J. H. Concerted Rotation in a Tertiary Aromatic Amide: Towards a Simple Molecular Gear. *Angew. Chem., Int. Ed.* **1998**, *37* (13−14), 1937−1939.
(29) Ahmed, A.; Bragg, R. A.; Clayden, J.; Lai, L. W.; McCarthy, C.; Pink, J. H.; Westlund, N.; Yasin, S. A. Barriers to Rotation about the Chiral Axis of Tertiary Aromatic Amides. *Tetrahedron* **1998**, *54* (43), 13277−13294.
(30) Ko, E.; Liu, J.; Perez, L. M.; Lu, G.; Schaefer, A.; Burgess, K. Universal Peptidomimetics. *J. Am. Chem. Soc.* **2011**, *133* (3), 462−477.
(31) Ko, E.; Raghuraman, A.; Perez, L. M.; Ioerger, T. R.; Burgess, K. Exploring Key Orientations at Protein-Protein Interfaces with Small Molecule Probes. *J. Am. Chem. Soc.* **2013**, *135* (1), 167−173.
(32) Xin, D.; Ko, E.; Perez, L. M.; Ioerger, T. R.; Burgess, K. Evaluating Minimalist Mimics by Exploring Key Orientations on Secondary Structures (EKOS). *Org. Biomol. Chem.* **2013**, *11* (44), 7789−7801.
(33) Douse, C. H.; Maas, S. J.; Thomas, J. C.; Garnett, J. A.; Cota, E.; Tate, E. W. Crystal Structures of Stapled and Hydrogen Bond Surrogate Peptides Targeting a Fully Buried Protein-Protein Interaction. *ACS Chem. Biol.* **2014**, *9* (10), 2204−2209.
(34) Grossmann, T. N.; Yeh, J. T.-H.; Bowman, B. R.; Chu, Q.; Moellering, R. E.; Verdine, G. L. Inhibition of oncogenic Wnt signaling through direct targeting of β-catenin. *Proc. Natl. Acad. Sci. U. S. A.* **2012**, *109* (44), 17942−17947.
(35) Takada, K.; et al. Targeted Disruption of the BCL9/β-catenin Complex Inhibits Oncogenic Wnt Signaling. *Sci. Transl. Med.* **2012**, *4* (148), 148ra117.
(36) Barba, A.; Dominguez, S.; Cobas, C.; Martinsen, D. P.; Romain, C.; Rzepa, H. S.; Seoane, F. Workflows Allowing Creation of Journal Article Supporting Information and Findable, Accessible, Interoperable and Reusable (FAIR)-Enabled Publication of Spectroscopic Data. *ACS Omega* **2019**, *4* (2), 3280−3286.

DOI: 10.1021/acs.orglett.9b01115
Org. Lett. 2019, 21, 4433−4438